



Spectroscopic, thermal analysis and DFT computational studies of salen-type Schiff base complexes



Hossein Pasha Ebrahimi^a, Jabbar S. Hadi^{b,*}, Zuhair A. Abdulnabi^b, Zeinab Bolandnazar^c

^a Department of Biochemistry and National Magnetic Resonance Facility at Madison (NMRFAM), University of Wisconsin-Madison, Madison, WI 53706, USA

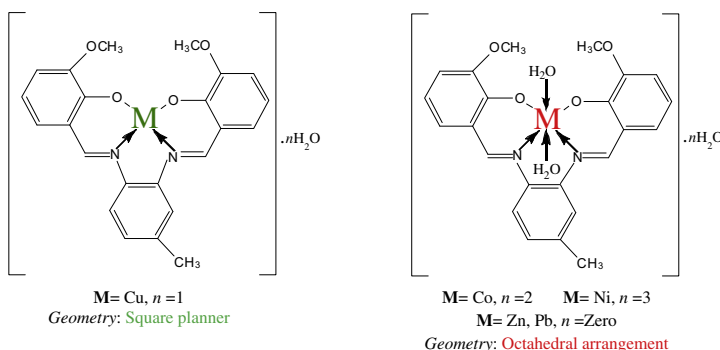
^b Department of Chemistry, College of Education for Pure Science, University of Basrah, Basrah, Iraq

^c School of Medicine, University of Wisconsin-Madison, Madison, WI 53706, USA

HIGHLIGHTS

- A tetradentate salen-type Schiff base and its metal complexes were synthesized.
- The spectral and thermal properties of these complexes were studied.
- Compounds were characterized by IR, UV–Vis, NMR, as well as mass spectroscopy.
- The TG analyses suggest high stability for all complexes.
- The theoretical calculations were performed using different DFT methods.

GRAPHICAL ABSTRACT



ARTICLE INFO

Article history:

Received 11 April 2013

Received in revised form 5 August 2013

Accepted 8 August 2013

Available online 24 August 2013

Keywords:

Salen-type Schiff base
Metal Schiff base complex
Tetradentate ligand
Octahedral geometry
Coats–Redfern
Phenylenediamine

ABSTRACT

A new series of metal(II) complexes of Co(II), Ni(II), Cu(II), Zn(II), and Pb(II) have been synthesized from a salen-type Schiff base ligand derived from *o*-vanillin and 4-methyl-1,2-phenylenediamine and characterized by elemental analysis, spectral (IR, UV–Vis, ¹H NMR, ¹³C NMR and EI-mass), molar conductance measurements and thermal analysis techniques. Coats–Redfern method has been utilized to calculate the kinetic and thermodynamic parameters of the metal complexes. The molecular geometry, Mulliken atomic charges of the studied compounds were investigated theoretically by performing density functional theory (DFT) to access reliable results to the experimental values. The theoretical ¹³C chemical shift results of the studied compounds have been calculated at the B3LYP, PBEPBE and PW91PW91 methods and standard 6-311+G(d,p) basis set starting from optimized geometry. The comparison of the results indicates that B3LYP/6-311+G(d,p) yields good agreement with the observed chemical shifts. The measured low molar conductance values in DMF indicate that the metal complexes are non-electrolytes. The spectral and thermal analysis reveals that all complexes have octahedral geometry except Cu(II) complex which can attain the square planner arrangement. The presence of lattice and coordinated water molecules are indicated by thermograms of the complexes. The thermogravimetric (TG/DTG) analyses confirm high stability for all complexes followed by thermal decomposition in different steps.

© 2013 Elsevier B.V. All rights reserved.

Introduction

As an important class of compounds, Schiff bases have received much attention in the wide variety of fields due to their different

applications owing to their characteristic properties such as pre-ferable accessibility, structural variety, varied coordinating ability, thermal stability, biological activities and catalysis properties [1–5]. In several decades, fruitful efforts have been made to design and synthesize Schiff bases and their complexes to apply these compounds in the different fields of study [6–9]. A variety of transition metal complexes with bi-, tri- and tetradentate Schiff bases

* Corresponding author. Tel.: +964 7710822193.

E-mail address: jshalkabi2@gmail.com (J.S. Hadi).

containing oxygen and nitrogen donor atoms are of particular interest, because of their ability to possess unusual configuration, and remarkable biomedical activities [10–14]. Salen-type Schiff base ligands as one of the oldest classes of ligands in coordination chemistry has been used extensively as the source of tetradentate ligands to complex transition metals [15–17]. This family of Schiff bases derived from aromatic or aliphatic diamine and phenolic aldehydes are the popular chelating ligands used in coordination chemistry. Since asymmetric Schiff base ligands have many advantages over their symmetrical counterparts in the composition and geometry of transition metal complexes and properties, salens are privileged ligands for application in asymmetric catalysis. Also, salen metal complexes have been successfully used as catalytic species in numerous organic transformations [18–20].

In connection of widely applications for Schiff base ligands and their metal complexes, we have synthesized and characterized a new series of metal(II) complexes of Co(II), Ni(II), Cu(II), Zn(II), and Pb(II) with a salen-type Schiff base ligand derived from *o*-vanillin and 4-methyl-1,2-phenylenediamine. The synthesized compounds have been characterized on the basis of spectroscopic methods including IR, UV–Vis, ^1H and ^{13}C NMR, and mass spectroscopy as well as elemental analyses and molar conductance measurements. We also utilized thermogravimetric (TG/DTG) analyses as the mostly used techniques and the widely applied Coats–Redfern calculation procedure for the kinetic analysis [21]. The kinetic and thermodynamic parameters have been calculated using Coats–Redfern method based on thermal data analysis. To additionally verify the proposed assignments, quantum chemical calculations have been performed. In order to make sense between the experimental and theoretical results, Mulliken atomic charges and ^{13}C NMR chemical shifts of the studied compounds were calculated and the results were discussed. In the present study, we have also extended the probing into the application of DFT methods. Therefore, these synthesized compounds have theoretically investigated by using various DFT methods including B3LYP, PBEPBE and PW91PW91 in 6-311+G(d,p) basis set. The theoretical ^{13}C chemical shift results were also calculated using the gauge independent atomic orbital (GIAO) approach and their respective linear correlations were obtained.

Experimental procedure

Materials

Analar grade metal salts were used as a source of metal for synthesis of the complexes. $\text{Cu}(\text{CH}_3\text{COO})_2 \cdot \text{H}_2\text{O}$, $\text{Zn}(\text{CH}_3\text{COO})_2$ and $\text{Pb}(\text{CH}_3\text{COO})_2$ as well as *o*-vanillin were obtained from Fluka. $\text{Co}(\text{NO}_3)_2 \cdot 6\text{H}_2\text{O}$, $\text{NiCl}_2 \cdot 6\text{H}_2\text{O}$ were obtained from BDH. 4-Methyl-1,2-phenylenediamine were obtained from Merck and used after recrystallization from water. All solvents employed in synthesis were of extra-pure grade and used as received without further purification.

Instrumentation and spectral measurements

IR spectra were recorded by using Shimadzu FTIR-8300 spectrophotometer in the region $4000\text{--}400\text{ cm}^{-1}$ in KBr pellet and in CCl_4 solution. The spectra were collected with a resolution of 2 cm^{-1} with 15 scans. The mass spectra for ligand were scanned by the EI technique at 70 eV with an Agilent Technologies 5975C spectrometer. The experimental values of ^1H and ^{13}C NMR spectra for the studied compounds were scanned on a Bruker Avance DX500 MHz spectrometer with a field gradient operating at 500.13 MHz for proton observation. TMS as the internal standard was used as referenced to 0.0 ppm. DMSO-d_6 , CDCl_3 were used as

solvents. The experiments were run in unlock mode, with sufficient a number of scans to achieve S/N ratios 200:1 (ca.). NMR spectra were obtained at a probe temperature of about 298 K. The UV–Vis spectra were recorded with a PG-T80⁺ spectrophotometer. Melting points were recorded on a Fisher Johns melting point apparatus. The metal content of the complexes was determined by a Buck Scientific's 210VGP Atomic Absorption Spectrophotometer. The molar conductance of complexes was measured using conductometer corning model 441. All measurements were performed at room temperature using DMF (10^{-3} M) as a solvent. The thermal analyses (TG and DTA) were carried out in dynamic nitrogen atmosphere (20 mL min^{-1}) with a heating rate of $10\text{ }^\circ\text{C min}^{-1}$ using a Perkin–Elmer thermal analyzer. Elemental analyses (C, N, and H) were performed in a CHNS-932 LECO apparatus.

Preparation methods

Synthesis of the H_2L Schiff base ligand

The Schiff base (H_2L), (6,6'-(4-methyl-1,2-phenylene)bis(azan-1-yl-1-ylidene)bis(2-methoxyphenol)), was prepared by mixing 50 mL of ethanolic hot solution ($60\text{ }^\circ\text{C}$) of 4-methyl-1,2-phenylenediamine (2.44 g, 20 mmol) with 50 mL hot ethanolic solution ($60\text{ }^\circ\text{C}$) of *o*-vanillin (6.08 g, 40 mmol) in the same solvent. Then, 2 drops of H_2SO_4 was added to make the medium acidic and the reaction mixture was stirred at $\sim 70\text{ }^\circ\text{C}$ for 30 min and was left under reflux for 2 h. The resulting orange precipitate solid was filtered, washed with ethanol and finally recrystallized from ethanol. The orange Schiff base product is produced in 80% yield. The synthesis of H_2L Schiff base was performed in accordance with reaction Scheme 1.

Synthesis of the transition metal complexes of the Schiff base

Co complex: (0.39 g, 1 mmol) of the Schiff base ligand (H_2L) was dissolved in 20 mL of warm ethanol and (0.291 g, 1 mmol) of $\text{Co}(\text{NO}_3)_2 \cdot 6\text{H}_2\text{O}$ in 20 mL of ethanol was added to it. The resulting mixture was refluxed after 2 h. The brown precipitate was washed with ethanol and diethyl ether, filtered, and dried in air.

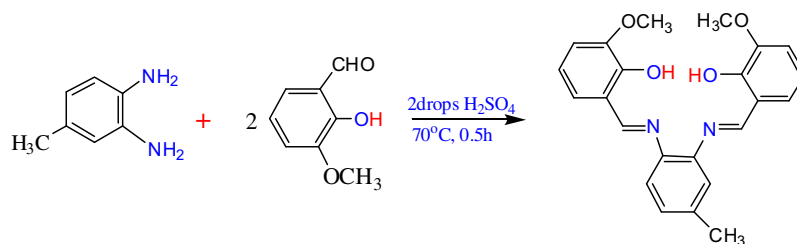
Ni complex: The Ni(II) complex was prepared in a similar procedure of the Co(II) complex by the addition of warm solution of $\text{NiCl}_2 \cdot 6\text{H}_2\text{O}$ (0.237 g, 1 mmol) in 20 mL of ethanol to the warm solution of the Schiff base ligand (0.39 g, 1 mmol) in the same solvent system. The resulting mixture was refluxed for 1 h to give a reddish brown powder.

Cu and Zn complex: The Cu(II) and Zn(II) complexes were prepared in a similar procedure of the Co(II) complex. (0.39 g, 1 mmol) of the Schiff base ligand (H_2L) was dissolved in 20 mL of warm ethanol and (0.199 g, 1 mmol) of $\text{Cu}(\text{CH}_3\text{COO})_2 \cdot \text{H}_2\text{O}$ in 20 mL of ethanol was added to it. The resulting mixture was refluxed after 3 h to give a brown powder. The Zn(II) complex was prepared by addition of the Schiff base (0.39 g, 1 mmol) in 20 mL of warm ethanol to (0.183 g, 1 mmol) of $\text{Zn}(\text{CH}_3\text{COO})_2$ in 20 mL of ethanol. The mixture was under reflux for 1 h to give a pale yellow pellicle.

Pb complex: (0.39 g, 1 mmol) of Schiff base ligand (H_2L) was dissolved in a solution of (0.08 g, 2 mmol) sodium hydroxide in 20 mL ethanol. The solution was heated in the water bath at $70\text{ }^\circ\text{C}$. (0.325 g, 1 mmol) of $\text{Pb}(\text{CH}_3\text{COO})_2$ in 20 mL of ethanol was added drop wise to it. The mixture then was refluxed for 2 h. The precipitate filtered and washed with hot ethanol and diethyl ether. The obtained orange pellicle was then dried in air.

Computational aspects

By increasing development of computational chemistry, density functional theory (DFT) has been extensively used due to their accuracy and low computational cost to calculate a wide variety



Scheme 1. Preparation of H_2L Schiff base ligand.

of molecular properties and provided reliable results which are in accordance with experimental data [22]. In present work, three popular DFT methods were used to perform theoretical calculations on the studied compounds. The methods include the Beck's three-parameter exchange functional [23] with Lee et al.'s correlation functional (B3LYP) [24]; Perdew and Wang's 1991 exchange with gradient-corrected correlation functional (PW91PW91) [25]; and Perdew et al.'s exchange and correlation functional (PBE/PBE) [26]. The geometry of all compounds was fully optimized at the B3LYP level of theory along with standard 6-311+G(d,p) basis set which has amply been proven to give very good ground-state geometries. No constraints were imposed on the structure during the geometry optimizations. The vibrational frequency analyses, calculated at the same level of theory, indicate that the optimized structures are at the stationary points corresponding to local minima without any imaginary frequency. The electronic properties and Mulliken atomic charges were calculated using mentioned DFT methods based on the optimized structures. In addition, a comparison was made between the theoretically calculated ^{13}C chemical shift constants and the experimentally measured ^{13}C chemical shifts. GIAO (Gauge Including Atomic Orbital) as the most widely used approach for calculating NMR shielding tensors were applied [27–33]. The Gaussian 09 package was employed to perform optimization of structures and all the calculations [34].

Results and discussion

Experimental results

In this section, spectral studies including the observed spectroscopic results for the title compounds are discussed.

Physical property

The observed physical properties of H_2L Schiff base ligand and its synthesized complexes are collected in Table 1. All Co(II), Ni(II), Cu(II), Zn(II) and Pb(II) complexes are colored, air stable in the solid state, having high melting points. These complexes are insoluble in most common organic solvents such as ethanol, acetone, diethyl ether, and methylene chloride but are readily soluble in DMF and DMSO. It is clear from the data that the experimental values shown for each of the compound are in good agreement with the theoret-

ical values calculated for 1:1 ratio. Also, the measured molar conductance values indicate the non-electrolytic nature of the complexes. Therefore, it seems that two phenolic OH have been deprotonated and bonded to the metal ions as oxygen anion. The complexes are as follow: $[Co(L)(H_2O)_2] \cdot 2H_2O$, $[Ni(L)(H_2O)_2] \cdot 3H_2O$, $[Cu(L)] \cdot H_2O$, $[Zn(L)(H_2O)_2]$, and $[Pb(L)(H_2O)_2]$.

Spectral characterization

A complete set of spectral data of the complexes is given in Supplementary data.

Mass spectra analysis

Mass spectrometry as a powerful structural characterization technique in coordination chemistry has been successfully used to confirm the molecular ion peaks of H_2L Schiff base and investigate the fragment species. The fragment pattern of mass spectrum gives an impression for the successive degradation of the target compound with the series of peaks corresponding to various fragments. Also, the peaks intensity gives an idea about the stability of fragments especially with the base peak. The recorded mass spectrum of H_2L Schiff base ligand reveals the molecular ion peak confirms strongly the condensation of *o*-vanillin with 4-methyl-1,2-phenylenediamine in 2:1 mol ratio and the proposed formula. The spectrum of the ligand displays the molecular ion peak at m/z 390 with relative abundance 69% which is agreement with the formula $C_{23}H_{22}N_2O_4$ and is equivalent to its molecular weight. It is also confirming the purity of the ligand prepared. The ligand shows some important peaks at m/z 375 (8%) corresponding to $[M-CH_3]^+$, and at m/z 373 (11%) belongs to $[M-OH]^+$. A peak at m/z 267 (10%) was observed as a result of loss of $C_7H_7O_2$ as well as loss of $C_8H_7O_2$ group from the ligand which was given fragment ion at m/z 254 (23%). All these peaks show an evidence of ligand formation.

IR spectra analysis

The IR spectrum of the free Schiff base ligand shows the medium and broad band at 3417 cm^{-1} that attributed to the OH stretching vibration as the main characteristic band. A strong band is observed at 1614 cm^{-1} which is assigned to $\nu(C=N)$ and a very strong band appeared at 1253 cm^{-1} in the free Schiff base ligand

Table 1
Physical properties of H_2L Schiff base and its metal complexes.

Compound	Physical state	Color, melting point (°C)	Yield (%)	M% found (Calc.)	C% found (Calc.)	N% found (Calc.)	H% found (Calc.)	λ ($\Omega^{-1}\text{ cm}^2\text{ mol}^{-1}$)
H_2L	Pellicle	O (180–181)	80	–	–	–	–	–
$[Co(L)(H_2O)_2] \cdot 2H_2O$	Powder	B (>300)	37	12.04 (11.36)	53.66 (53.18)	5.62 (5.39)	5.68 (5.43)	34.10
$[Ni(L)(H_2O)_2] \cdot 3H_2O$	Powder	R-B (280 days)	49	12.66 (11.60)	51.39 (55.12)	5.59 (5.21)	5.81 (5.58)	9.81
$[Cu(L)] \cdot H_2O$	Powder	B (279–280)	40	11.45 (13.43)	58.16 (58.78)	6.08 (5.96)	4.91 (4.72)	0.57
$[Zn(L)(H_2O)_2]$	Pellicle	P-Y (>300)	88	11.97 (13.29)	55.41 (56.39)	6.11 (5.72)	5.06 (4.94)	0.20
$[Pb(L)(H_2O)_2]$	Pellicle	D-O (>300)	81	33.19 (32.58)	43.18 (43.73)	4.07 (3.83)	4.07 (3.83)	10.93

O: orange, P-Y: pale yellow, R-B: reddish brown, B: brown, D-O: dark orange.

is attributed to $\nu(\text{C}=\text{O})$. Also, coordination of the Schiff base to the metal ions through the nitrogen atom is expected to reduce electron density in the azomethine link and lower the $\nu(\text{C}=\text{N})$ absorption frequency. This band at 1614 cm^{-1} in the free Schiff base ligand is shifted to a lower wave number side ($\Delta\nu \sim 2\text{--}14\text{ cm}^{-1}$) in all the complexes indicates the participation of the azomethine groups in coordination to the metal ions through the lone pair of electrons on the nitrogen. This peak is appeared at 1600 cm^{-1} for Cu(II) complex. In addition, the involvement of phenolic OH groups in bonding with the metal ions can be examined by the $\nu(\text{C}=\text{O})$ band which is shifted to lower wave number side. Furthermore, the new weak non-ligand bands in the region $540\text{--}588$ and $428\text{--}459\text{ cm}^{-1}$ in the spectra of the complexes are assigned to stretching frequencies of $\nu(\text{M}=\text{O})$ and $\nu(\text{M}=\text{N})$ bonds, respectively [35]. This indicates that phenolic oxygen and azomethine nitrogen atoms are involved in coordination.

Electronic spectral analysis

The electronic absorption spectra of the Schiff base ligand and the metal complexes under investigation were recorded within the range $350\text{--}800\text{ nm}$. The data of electronic spectrum of **H₂L** Schiff base ligand was collected in DMF solvent with five absorption bands at $546, 396, 352, 334$ and 308 nm . The spectral bands at 308 and 334 nm were assigned to transition motions of phenyl rings [36]. The transition band at 352 nm corresponded to $n \rightarrow \pi^*$ transition of azomethine group $-\text{CH}=\text{N}$, while, the bands at 396 and 546 nm assigned to $n \rightarrow \pi^*$ transitions of donating atoms like oxygen and nitrogen which are overlapped with the intermolecular L_{CT} from aromatic rings. The peaks within the transition motions of phenyl rings have been relatively unaffected in the spectra of the complexes; this is expected for the relatively unshared of aromatic ring in chelation. The transition bands up to 350 nm which assigned to $n \rightarrow \pi^*$ transition due to involving molecular orbitals of the $-\text{CH}=\text{N}$ chromophore. In the spectra of the complexes (except Cu(II) complex), the bands of the azomethine chromophore bands (the bands of $n \rightarrow \pi^*$ transition) are shifted to lower frequencies or lost, indicating that the imine nitrogen atom is involved in coordination to the metal ion. The electronic spectrum of the Cu(II) complex exhibits two bands at 545 and 438 nm corresponding to ${}^2\text{B}_{1g} \rightarrow {}^2\text{E}_g$ and ${}^2\text{B}_{1g} \rightarrow {}^2\text{A}_{1g}$ transitions in a square planar geometry. Also, based on previous studies of salen-type Schiff bases, the Co(II) shows a more pronounced tendency than Co(III) for the reaction with this type of Schiff bases and the formation of octahedral structure in the presence of addition donors [37,38]. However, in general, relatively strong π -acceptor ligands (such as pyridine and its derivatives, or anions such as N_3 , and CN) increase effectively the ligand field strength to facilitate the oxidation of the Co(II) and the formation of Co(III) with an octahedral structure.

${}^1\text{H}$ and ${}^{13}\text{C}$ NMR spectra analysis

The ${}^1\text{H}$ NMR spectral data of the Schiff base ligand at ambient temperature in $\text{DMSO-}d_6$ confirms the proposed structural elucidation of the ligand **H₂L**. This ${}^1\text{H}$ NMR spectrum of the Schiff base ligand shows the methyl protons as a singlet signal at $\delta \sim 2.3\text{ ppm}$. It also displays a singlet signal at $\delta \sim 3.8\text{ ppm}$ which is attributed to protons of two methoxy groups of vanillin moiety. The two azomethine protons appear at $\delta \sim 8.91\text{ ppm}$. The signals at $\delta \sim 12.99$ and 13.11 ppm are attributed to two non-equivalent OH protons. The disappearance of these phenolic proton signals from the ${}^1\text{H}$ NMR spectra of all complexes, supports the proton displacement from the OH groups through the metal ions. A comparison of the chemical shifts of the ligand with its complexes such as Zn(II) and Ni(II) complexes indicates that the signals due to phenolic protons are absent in the complexes spectra. This can be attributed due to the deprotonation of the phenolic groups and subsequently the replacement of the protons by metal. The azomethine proton sig-

nals are observed upfield at $\delta \sim 8.7\text{ ppm}$ and 8.81 ppm in case of Zn(II) complex and are shifted downfield at $\delta \sim 8.97$ and 8.99 ppm in Ni(II) complex. It supports the coordination of azomethine nitrogen to metal ion. Therefore, the ${}^1\text{H}$ NMR result supports the assigned geometry.

The measured chemical shifts of all carbon atoms for ligand and Zn complex spectra as a case study of complexes are listed in Table 2, where the numbering of the carbon atoms is presented only for ${}^{13}\text{C}$ NMR data assignment in Fig. 1. Also, magnetically equivalent carbons are displayed by same number. The ${}^{13}\text{C}$ NMR spectrum of the Zn(II) complex in DMSO is depicted in Fig. 2. As shown in Fig. 2, the two azomethine carbon signals appear at ~ 164.18 and 163.52 ppm . These two signals are shifted upfield in Zn(II) complex spectrum which indicates the participation of azomethine groups in complex formation. The signal of carbon attached to hydroxyl groups (C_4, C'_4) in **H₂L** Schiff base ligand appears at $\delta \sim 148.59\text{ ppm}$. This signal is shifted to $\delta \sim 139.56\text{ ppm}$ in Zn(II) complex spectrum due to bonding formation between oxygen and metal ion. On the basis of electronic spectra, the following thermal pattern, and the previous studies of Zn(II) structures, an octahedral geometry around Zn(II) is suggested [38–40]. Then, based on the above spectroscopic data the following structures are proposed for complexes in Fig. 3.

Thermal analysis

Thermal analyses (TG and DTG) of the Schiff base ligand and its complexes were used to get information about the thermal stability of these new complexes as well as to verify the status of water molecules into inside or outside the inner coordination sphere of the central metal ion. The complexes were subjected to a TG analysis ambient temperature up to $800\text{ }^\circ\text{C}$ under nitrogen atmosphere with heating rate $10\text{ }^\circ\text{C}/\text{min}$. The mass losses obtained from TG curves are in a good agreement with the calculated values. The decomposition pathways of all complexes which vary from one complex to another confirm suggested structures of Fig. 3. *Co complex*: Co complex undergoes decomposition in four steps. The first decomposition step is accompanied by weight loss (Obs. = 6.81% , Calc. = 6.89%) which assigned to the loss of two lattice water molecules. The second step shows loss in weight within the temperature range of $130\text{--}210\text{ }^\circ\text{C}$, which is due to removal of one coordinated water molecule. The third decomposition step represents the loss of another coordinated water molecule and it indicates that the two coordinated water molecules are energetically nonequivalent. The fourth step seems to be composed of two overlapping steps as indicated from DTG curve (at 285 and $375\text{ }^\circ\text{C}$). The remaining product at $\sim 380\text{ }^\circ\text{C}$ is identified as CoO (Obs. = 14.53% ,

Table 2
 ${}^{13}\text{C}$ chemical shifts (in ppm) for **H₂L** Schiff base and Zn complex.

No. carbon atom	H ₂ L	Zn complex
C1	164.1	163.01
C2	163.5	162.4
C3,3'	151.5	152.96
C4,4'	148.5	139.56
C5	142.3	137.47
C6	140.1	137.28
C7	137.72	128.33
C8	128.11	127.79
C9	123.88	120.3
C10	123.8	119.17
C11,11'	121.03	117.04
C12,12'	119.8	116.53
C13,13'	115.03	114.22
C14,14'	118.4	112.24
C15,15'	56.14	55.6
C16	21.06	21.4

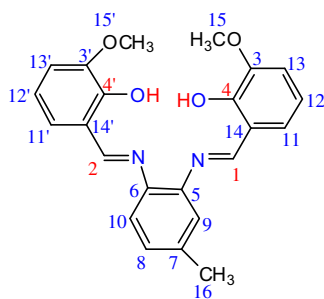


Fig. 1. Structure of H_2L Schiff base with the numbering of the carbon atoms (which is only for ^{13}C NMR data assignments in Table 2).

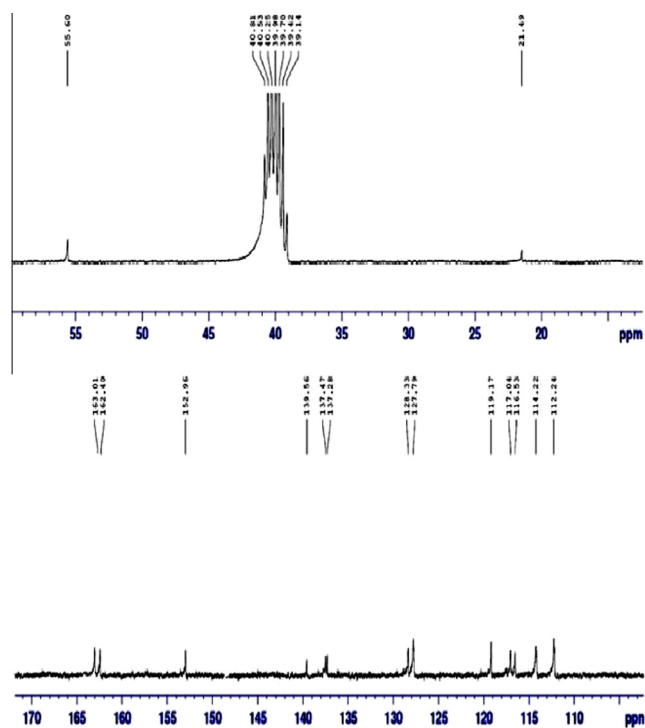


Fig. 2. ^{13}C NMR spectra of Zn(II) complex.

Calc. = 14.45%). *Ni complex*: The first decomposition step seems to be composed of two overlapping steps as indicated from DTG curve (at 90 and 165 °C) corresponds to the release of two lattice waters.

The second step in the range of 175–225 °C has a total weight loss (Obs. = 3.8%, Calc. = 3.73%) assigned to the evolved the third lattice water. The third step corresponds to loss coordinated water molecules in the range of 230–320 °C. The next step represents the decomposition of the ligand and the remaining product at 640 °C could be identified as NiO polluted with 3 carbon atoms (Obs. 21.84%, Calc. 21.84%). *Cu complex*: The TGA curve of Cu(II) complex displays two stages of mass loss which the first step corresponds to release one lattice water molecule (Obs. = 3.76%, Calc. = 3.82%) and the next step represents the decomposition of the ligand parts. The remaining product is CuO. (Obs. = 16.71%, Calc. = 16.84%). *Zn complex*: This complex was stable up to 155 °C and no weight loss was detected. It means that the complex is anhydrous. The first two decomposition steps correspond to loss two coordinated water molecules. The third step within the temperature range of 350–465 °C represents a decomposition of ligand parts, may be two methanol molecules (Obs. = 13.56%, Calc. = 14.12%). The remaining weight was 16.53% which represents to ZnO (Calc. = 16.56%). *Pb complex*: No weight loss was observed until 220 °C which is confirmed that the complex is anhydrous. The TGA curve of Pb(II) complex shows loss in weight (Obs. = 5.43%, Calc. = 5.7%), which is due to removal of two coordinated water molecules. The remaining product is identified as PbO (Obs. = 36.66%, Calc. = 36.7%).

Kinetic and thermodynamic data analysis

The thermal dehydration and decomposition of the mentioned complexes were studied kinetically using the integral method applying the Coats–Redfern method [41]. The thermodynamic activation parameters of decomposition processes of dehydrated complexes namely activation energy (E), frequency factor (A), enthalpy of activation (ΔH), entropy of activation (ΔS), and Gibbs free energy change of the decomposition (ΔG) are evaluated graphically from TG and DTG data by employing the Coats–Redfern relation in the following form:

$$\log \left[\frac{\log \frac{W_f}{W_f - W_t}}{T^2} \right] = \log \left[\frac{AR}{\theta E} \left(1 - \frac{2RT}{E} \right) \right] - \frac{E}{2.303RT} \quad (1)$$

where W_f , W_t are weight loss at the end of stage and weight loss at temp (t), respectively. Also, E , R , A , θ are the activation energy, the universal gas constant, pre-exponential factor and heating rate (10 °C/min), respectively. In the present work, the decomposition stages of all complexes show a best fit for first order reaction in all stages. The correlation coefficient, r , was computed using the least square method by plotting the left-hand side of Eq. (1), versus $1000/T$. (Figure of the first step of decomposition of Cu(II) complex is shown in Supplementary data.) The thermo-kinetic data are summarized in Table 3. The high values of the activation energies reflect

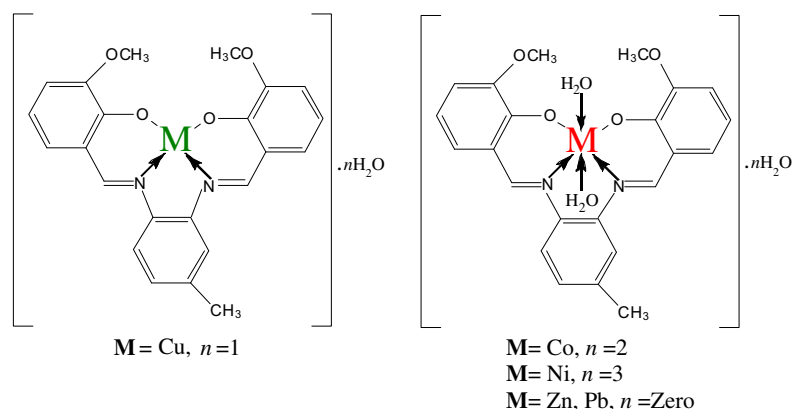


Fig. 3. Suggested structure of metal complexes.

Table 3
Kinetic parameters of the complexes using the Coats–Redfern equation.

Compound	Step	A (s^{-1})	E ($kJ\ mol^{-1}$)	ΔH ($kJ\ mol^{-1}$)	ΔS ($J\ mol^{-1}\ K^{-1}$)	ΔG ($kJ\ mol^{-1}$)	r
[Co(L)(H ₂ O) ₂]-2H ₂ O	1st	8.57×10^3	46.173	43.030	-0.1715	107.89	0.990
	2nd	1.47×10^{22}	275.617	272.100	0.368	116.43	0.991
	3rd	1.86×10^{23}	348.369	344.145	0.3875	147.257	0.967
	4th	1.88×10^8	129.052	124.163	-0.0921	178.354	0.999
[Ni(L)(H ₂ O) ₂]-3H ₂ O	1st	1.59×10^9	78.721	75.703	-0.434	233.279	0.987
	2nd	1.01×10^9	97.375	93.733	-0.439	286.202	0.986
	3rd	1.03×10^{24}	268.155	263.723	0.210	151.789	0.996
	4th	5.16×10^{13}	230.904	224.478	0.0096	216.986	0.993
[Cu(L)]-H ₂ O	1st	1.67×10^3	40.990	37.838	-0.1851	108.023	0.994
	2nd	4.94×10^{17}	236.921	231.907	0.0879	178.866	0.985
	3rd	2.51×10^5	125.560	119.133	-0.1494	234.646	0.993
[Zn(L)(H ₂ O) ₂]	1st	3.24×10^{14}	153.419	149.37	0.0288	135.363	0.991
	2nd	1.80×10^{25}	432.45	427.436	0.424	171.66	0.996
	3rd	8.40×10^{15}	229.419	224.07	0.0535	189.646	0.967
	4th	8.47×10^{19}	306.038	300.168	0.1294	208.81	0.966
[Pb(L)(H ₂ O) ₂]	1st	1.39×10^3	37.037	34.310	-0.1855	95.156	0.963
	2nd	2.35×10^5	92.145	87.432	-0.1474	171.164	0.993
	3rd	5.04×10^{27}	345.244	340.314	0.2797	174.451	0.989
	4th	1.83×10^{15}	220.136	214.666	0.0406	187.893	0.996
	5th	1.44×10^{17}	266.649	260.762	0.0763	206.691	0.993

the thermal stability of the complexes and also are supported the reaction to proceed slower than normal [42]. The entropy of activation values are positive in most of investigated temperature ranges indicating dissociation character of decompositions. In some temperature ranges, the entropy of activation is found to have very low values or negative values which indicate that the decomposition reactions process occur at very low rate. It also revealed the activated complex has a more ordered than that of either the reactants [43]. In addition, the positive values of (ΔH) means that the decomposition processes are endothermic. All values of ΔG are positive which indicate that all steps are nonspontaneous. This fact has been applicable for the **H₂L** complexes studied in the present paper.

Computational results

As mentioned before, all calculation carried out in the popular DFT methods (B3LYP, PBEPBE and PW91PW91) in 6-311+G(d,p)

basis set. The results are discussed for Schiff base ligand (**H₂L**) and Zn(II) complex as a case study and results for other Schiff base complexes are given in [Supplementary data](#). The optimized structure of **H₂L** along with labeling of atoms is shown in [Fig. 4](#). The figure shows the Schiff base ligand in the ball and stick model. The geometry optimization yields nonplanar structure. Also, the most optimized structural parameters of **H₂L** Schiff base ligand calculated by B3LYP/6-311+G(d,p) are presented in [Supplementary data](#).

Mulliken population analysis

The Mulliken analysis is the most common population analysis method. Mulliken atomic charge calculation has a significant role in the application of quantum chemical calculations to molecular systems because of atomic charges affect some properties of molecular systems including dipole moment, and molecular polarizability. The total atomic charge values of **H₂L** obtained by Mulliken population analysis [44] and illustration of atomic charges plotted is shown in [Fig. 5](#). The charge changes with methods

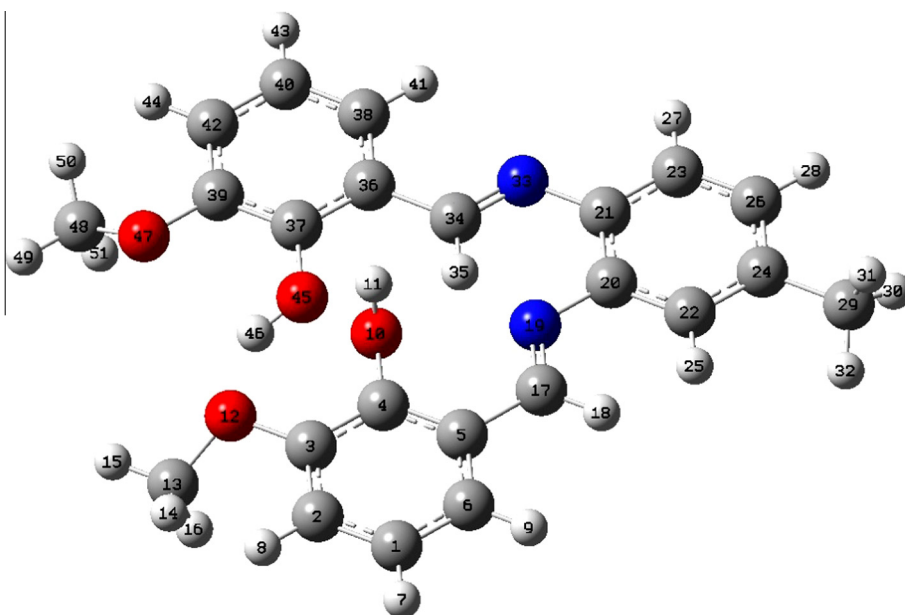


Fig. 4. The optimized structure of **H₂L** Schiff base ligand within numbering of atoms.

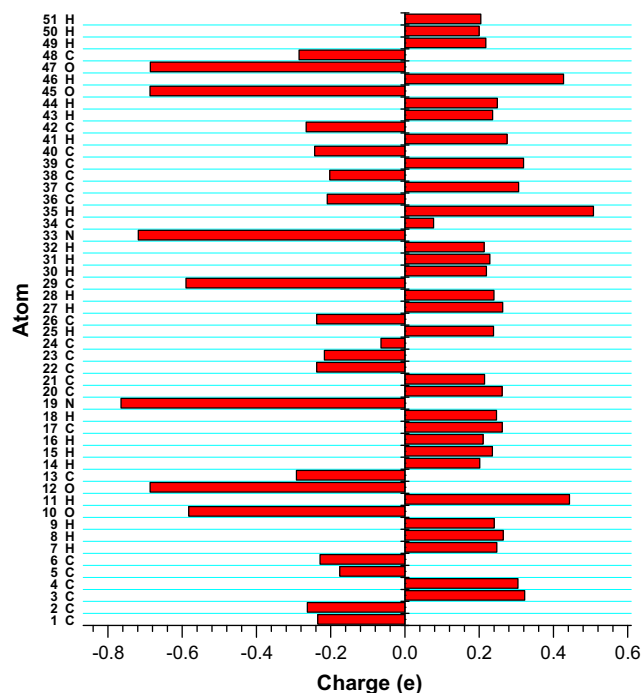


Fig. 5. The Mulliken atomic charge distribution of H₂L Schiff base.

Table 4
Statistical parameters of experimental versus theoretical ¹³C chemical shifts.

Method	Slope	Intercept	Correlation
<i>H₂L</i>			
B3LYP	0.9706	3.912	0.9937
PBEPBE	0.9651	4.184	0.9906
PW91PW91	0.9435	7.632	0.9878
<i>[Zn(L)(H₂O)₂]</i>			
B3LYP	0.9070	0.945	0.9805
PBEPBE	0.9057	1.978	0.9775
PW91PW91	0.9007	1.104	0.9703

presumably occur due to variation of the hybrid functionals. As can be seen in Fig. 5, all the hydrogen atoms have a net positive charge. The obtained atomic charge shows that the (H35) atom has bigger positive atomic charge (0.5077e) than the other hydrogen atoms. This is due to the presence of imine group. As expected, the results indicate that the charge of the nitrogen atom (N33) in imine group is negative. In addition, the results illustrate that the charge of the oxygen atoms in phenolic groups exhibits a negative charge, which are donor atoms. The results also show that the (H11) atom has more positive atomic charge (0.4430e) than the other hydrogen atoms. This is due to the presence of electronegative oxygen atom (O10), the hydrogen atom (H11) attracts the positive charge from the oxygen atom (O10) in phenolic group. Moreover, Mulliken atomic charges also confirm that an (H46) atom in phenolic ring is more acidic due to more positive charge.

NMR analysis

In order to comparison between experimental and theoretical NMR data, which may be helpful in making correct assignments and understanding the relationship between chemical shift and molecular structure, ¹³C NMR chemical shifts calculation for further clarification of synthesized Schiff base ligand and its complexes are reported. To clarify the relation between theoretical

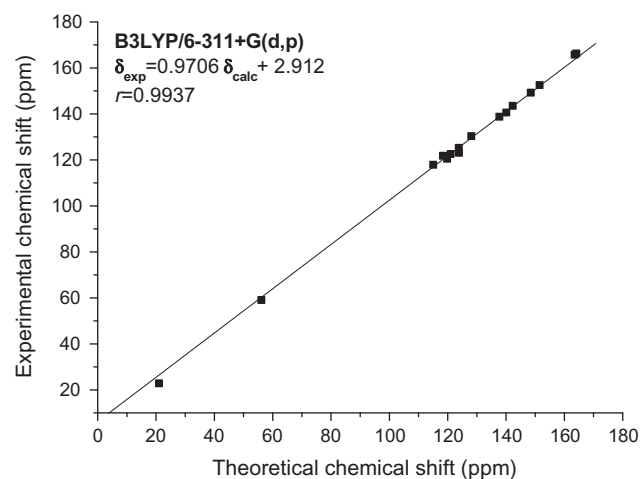


Fig. 6. Experimental values versus theoretical ¹³C NMR chemical shifts of H₂L Schiff base.

and experimental values of NMR chemical shift constants, the experimental data are plotted versus computed values.

The ¹³C NMR chemical shifts of all carbons were calculated on the optimized structures of compounds using mentioned DFT methods employing 6-311+G(d,p) basis set for all atoms. The impact of the solvent was taken into account using the Polarized Continuum Model (PCM) [45]. In order to compute the ¹³C NMR chemical shifts, each couple of carbon atoms on equivalent locations of the compound were considered as equivalent and their average of chemical shifts were calculated. The isotropic ¹³C chemical shifts calculated by all DFT methods are given in [Supplementary data](#) and compared with the experimental values. The statistical parameters of computed ¹³C NMR chemical shifts at the B3LYP/6-311+G(d,p), PBEPBE/6-311+G(d,p) and PW91PW91/6-31+G(d,p) levels of theory along with experimental data for Schiff base ligand (H₂L) and Zn(II) complex are given in Table 4. As can be seen, the results obtained by using all methods are in reasonable agreement with experimental values. The chemical shift changes with methods presumably occur due to variation of the hybrid functionals. The results of B3LYP method are closer to experimental data and they differ slightly from results of experiment. As shown in Fig. 6, there is a good linear relationship between experimental and theoretical B3LYP/6-311+G(d,p) chemical shifts.

Conclusion

The Schiff bases have been most widely used versatile ligands, in their neutral or deprotonated forms to form stable complexes with most of the transition metal ions. The work described in this paper involved the synthesis and spectroscopic as well as thermal characterization of a series of Co(II), Ni(II), Cu(II), Zn(II), and Pb(II) complexes with a novel tetradentate salen-type Schiff base ligand derived from 4-methyl-1,2-phenylenediamine, and *o*-vanillin, namely, (6,6'-(4-methyl-1,2-phenylene)bis(azan-1-yl-1-ylidene)bis(2-methoxyphenol)). Spectroscopic techniques including IR, UV–Vis, ¹H and ¹³C NMR, and mass analysis as well as elemental analysis and molar conductance measurement were used to identify the products. To study the structural and electronic properties of studied molecules, complete analyses of thermal decomposition of complexes and the ¹³C NMR spectra, as well as some kinetic and thermodynamic properties of all complexes was reported. All theoretical calculations were carried out by popular DFT methods including B3LYP, PBEPBE and PW91PW91 at 6-311+G(d,p) level

of theory. All applied methods are in good accordance with experimental values, especially results calculated by B3LYP/6-311+G(d,p). The consistency between the calculated and experimental NMR data indicates that B3LYP/6-311+G(d,p) method can generate reliable geometry and related NMR results of the title compounds. The kinetic and thermodynamic parameters as important values for stability index revealed high chemical reactivity of synthesized compounds in chemical reactions.

Appendix A. Supplementary material

Supplementary data associated with this article can be found, in the online version, at <http://dx.doi.org/10.1016/j.saa.2013.08.044>.

References

- [1] M.S. Refat, M.Y. El-Sayed, A.M. Adam, *J. Mol. Struct.* 1038 (2013) 62–72.
- [2] G. Gümrükçü, G.K. Karaoğlan, A. Erdoğan, A. Gül, U. Avcıata, *Dyes Pigm.* 95 (2012) 280–289.
- [3] K.C. Gupta, A. Kumar Sutar, C.-C. Lin, *Coord. Chem. Rev.* 253 (2009) 1926–1946.
- [4] S. Brooker, S.S. Iremonger, P.G. Pliedger, *Polyhedron* 22 (2003) 665–671.
- [5] S.N. Pandeya, D. Sriram, G. Nath, E. Declercq, *Eur. J. Pharmacol.* 9 (1999) 25–31.
- [6] M. Hanif, Z.H. Chohan, *Spectrochim. Acta A* 104 (2013) 468–476.
- [7] R.A. Ahmadi, S. Amani, *Molecules* 17 (2012) 6434–6448.
- [8] G.G. Mohamed, M.A. Zayed, S.M. Abdallah, *J. Mol. Struct.* 979 (2010) 62–71.
- [9] H. Ebrahimi, J.S. Hadi, H.S. Al-Ansari, *J. Mol. Struct.* 1039 (2013) 37–45.
- [10] A. Kakanejadifard, F. Esna-Ashari, P. Hashemi, A. Zabardasti, *Spectrochim. Acta A* 106 (2013) 80–85.
- [11] A. Golcu, M. Tumer, H. Demirelli, R.A. Wheatley, *Inorg. Chim. Acta* 358 (2005) 1785–1797.
- [12] A.D. Tiwari, A.K. Mishra, S.B. Mishra, B.B. Mamba, B. Maji, S. Bhattacharya, *Spectrochim. Acta A* 79 (2011) 1050–1056.
- [13] H. Keypour, M. Shayesteh, M. Rezaeiava, F. Chalabian, Y. Elerman, O. Buyukgungor, *J. Mol. Struct.* 1032 (2013) 62–68.
- [14] A.M. Tawfik, M.A. El-Ghamry, S.M. Abu-El-Wafa, N.M. Ahmed, *Spectrochim. Acta A* 97 (2012) 1172–1180.
- [15] A. Huber, L. Muller, H. Elias, R. Klement, M. Valko, *Eur. J. Inorg. Chem.* 2005 (2005) 1459–1467.
- [16] E.J. Campbell, S.T. Nguyen, *Tetrahedron Lett.* 42 (2001) 1221–1225.
- [17] A.W. Kleij, *Eur. J. Inorg. Chem.* 2009 (2009) 193–205.
- [18] A. Berkessel, M. Brandenburg, E. Leitterstorf, J. Frey, J. Lex, M. Schäfer, *Adv. Syn. Catal.* 349 (2007) 2385–2391.
- [19] T.A. Alsalm, J.S. Hadi, E.A. Al-Nasir, H.S. Abbo, S.J.J. Titinchi, *Catal. Lett.* 136 (2010) 228–233.
- [20] P.G. Cozzi, *Chem. Soc. Rev.* 33 (2004) 410–421.
- [21] R. Ebrahimi-Kahrizangi, M.H. Abbasi, *Trans. Nonferr. Met. Soc. China* 18 (2008) 217–221.
- [22] W. Koch, M.C. Holthausen, *A Chemist's Guide to Density Functional Theory*, second ed., Wiley, Weinheim, 2001.
- [23] A.D. Becke, *J. Chem. Phys.* 98 (1993) 5648–5652.
- [24] C. Lee, C. Hill, N. Carolina, *Phys. Rev. B* 37 (1988) 785–789.
- [25] J. Perdew, K. Burke, Y. Wang, *Phys. Rev. B* 54 (1996) 533–539.
- [26] J. Perdew, K. Burke, M. Ernzerhof, *Phys. Rev. Lett.* 77 (1996) 3865–3868.
- [27] H.P. Ebrahimi, H. Shaghghi, M. Tafazzoli, *Conc. Magn. Reson.* 38 A (2011) 269–279.
- [28] H.P. Ebrahimi, M. Tafazzoli, *Conc. Magn. Reson.* 40 A (2012) 192–204.
- [29] H.P. Ebrahimi, M. Tafazzoli, *Conc. Magn. Reson.* 42 A (4) (2013) 140–153.
- [30] H. Shaghghi, H. Ebrahimi, M. Tafazzoli, M. Jalali-Heravi, *J. Fluorine Chem.* 131 (2010) 47–52.
- [31] H. Shaghghi, H.P. Ebrahimi, N. Bahrami Panah, M. Tafazzoli, *Solid State Nucl. Magn. Reson.* 51–52 (2013) 31–36.
- [32] H. Shaghghi, F. Fathi, H.P. Ebrahimi, M. Tafazzoli, *Conc. Magn. Reson.* 42A (2013) 1–13.
- [33] M. Tafazzoli, H.P. Ebrahimi, *Phosphorus, Sulfur Silicon Relat. Elem.* 186 (2011) 1491–1500.
- [34] M.J. Frisch, G.W. Trucks, H.B. Schlegel, G.E. Scuseria, M.A. Robb, J.R. Cheeseman, G. Scalmani, V. Barone, B. Mennucci, G.A. Petersson, H. Nakatsuji, M. Caricato, X. Li, H.P. Hratchian, A.F. Izmaylov, J. Bloino, G. Zheng, J.L. Sonnenberg, M. Hada, M. Ehara, K. Toyota, R. Fukuda, J. Hasegawa, M. Ishida, T. Nakajima, Y. Honda, O. Kitao, H. Nakai, T. Vreven, J.A. Montgomery, Jr., J.E. Peralta, F. Ogliaro, M. Bearpark, J.J. Heyd, E. Brothers, K.N. Kudin, V.N. Staroverov, R. Kobayashi, J. Normand, K. Raghavachari, A. Rendell, J.C. Burant, S.S. Iyengar, J. Tomasi, M. Cossi, N. Rega, J.M. Millam, M. Klene, J.E. Knox, J.B. Cross, V. Bakken, C. Adamo, J. Jaramillo, R. Gomperts, R.E. Stratmann, O. Yazyev, A.J. Austin, R. Cammi, C. Pomelli, J.W. Ochterski, R.L. Martin, K. Morokuma, V.G. Zakrzewski, G.A. Voth, P. Salvador, J.J. Dannenberg, S. Dapprich, A.D. Daniels, Ö. Farkas, J.B. Foresman, J.V. Ortiz, J. Cioslowski, D.J. Fox, *Gaussian 09, Revision A.1*, Gaussian, Inc., Wallingford, CT, 2009.
- [35] K. Nakamoto, *Infrared and Raman Spectra of Inorganic and Coordination Compounds: Part A: Theory and Applications in Inorganic Chemistry*, sixth ed., John Wiley & Sons, Inc., New York, 2009.
- [36] A.B. Lever, *Inorganic Electronic Spectroscopy*, second ed., Elsevier, Amsterdam, 1997.
- [37] R. Vafazadeh, M. Kashfi, *Bull. Korean Chem. Soc.* 28 (2007) 1227–1230.
- [38] S. Bellemin-Laponnaz, S. Dagorne, in: J. Zabicky (Ed.), *PATAI's Chemistry of Functional Groups*, John Wiley & Sons, Ltd., New York, 2012, pp. 1–47.
- [39] E.T. Cavalheiro, F.C. Lemos, J.Z. Schpector, E.R. Dockal, *Thermochim. Acta* 370 (2001) 129–133.
- [40] K. Mounika, A. Pragathi, C. Gyanakumari, *J. Sci. Res.* 2 (2010) 513–524.
- [41] R.J. Coats AW, A.W. Coats, *Nature* 201 (1964) 68–69.
- [42] S.S. Sawhney, A.K. Bansal, *Thermochim. Acta* 66 (1983) 347–350.
- [43] A.A. Frost, R.G. Pearson, *Kinetics and Mechanism*, second ed., Wiley, New York, 1961.
- [44] R.S. Mulliken, *J. Chem. Phys.* 23 (1955) 1833–1840.
- [45] V. Barone, M. Cossi, J. Tomasi, *J. Chem. Phys.* 107 (1997) 3210–3221.